AJNR

The evolution of multiple sclerosis lesions on serial MR.

C R Guttmann, S S Ahn, L Hsu, R Kikinis and F A Jolesz

This information is current as of August 9, 2025.

The Evolution of Multiple Sclerosis Lesions on Serial MR

Charles R. G. Guttmann, Sungkee S. Ahn, Liangge Hsu, Ron Kikinis, and Ferenc A. Jolesz

PURPOSE: To characterize temporal changes in signal intensity patterns of multiple sclerosis lesions on serial MR. **METHODS:** T1-, T2-, proton density–, and contrast-enhanced T1-weighted MR was performed on five patients with relapsing-remitting multiple sclerosis at least 22 times in the course of 1 year. **RESULTS:** Forty-three enhancing lesions and 1 new lesion that never showed enhancement were detected and followed for periods ranging from approximately 4 weeks to 1 year (total of 702 time points). At first detection the center of new lesions was brighter than the periphery (20 of 24 new lesions on proton density–weighted and 19 of 23 new lesions on contrast-enhanced images). On contrast-enhanced images, ring hyperintensity was predominant at time points later than 29 days. As lesions aged, a residual rim of "nonenhancing" hyperintensity often was noted on contrast-enhanced images. Some older lesions (>1 year) showed similar appearance on unenhanced T1-weighted images. On proton density–weighted images ring hyperintensity was most frequent 2 to 4 months after lesion detection. The estimated average duration of gadopentetate dimeglumine enhancement was 1 to 2 months. **CONCLUSIONS:** A lesion evolution pattern relevant to MR was inferred. We believe that specific information about the histopathologic evolution of a lesion may be extracted not only from contrast-enhanced but also from nonenhanced serial MR. Assessment of drugs targeting specific phases of lesion evolution could benefit from quantitative pattern analysis of routine MR images.

Index terms: Sclerosis, multiple; Brain, magnetic resonance

Direct correlation of the magnetic resonance (MR) appearance of focal brain lesions in multiple sclerosis to histopathologic findings has been reported (1–5), albeit only occasionally, because of the difficulty in obtaining MR-correlated biopsy or autopsy samples. The histologic course of the disease has been so far inferred mainly from the heterogeneous appearance of lesions on postmortem specimens (6) and from animal studies of experimental allergic encephalitis (7–10). From such studies, it appears that focal lesions evolve in a concentric fashion. This lesion evolution is associated with changes in concentration and compartmentation of water and lipid protons and therefore could possibly be reflected on routine MR images. In this paper, we present an analysis of the appearance of individual white matter abnormalities in multiple sclerosis, as observed on serially acquired MR studies. We have followed 44 distinct white matter MR abnormalities for periods ranging from approximately 4 weeks to 1 year (total of 702 time points). Two independent observers described the MR appearance of these lesions at each time point by distinguishing lesions with a hyperintense center from lesions with a dark center surrounded by a brighter ring. The findings are discussed here in the light of neuropathologic and MR studies reported in the literature. In vivo determination of lesion composition and of changes therein could improve the understanding of multiple sclerosis pathogenesis and allow an MR-based classification of multiple sclerosis manifestation that is more re-

flective of distinct disease mechanisms, stages, and prognosis.

Methods

Patients

The subjects of this work were the first to complete a larger prospective follow-up study of 46 multiple sclerosis patients. Five patients with clinically ascertained relapsing-remitting multiple sclerosis were included in this analysis: 4 women and 1 man, with ages ranging from 27 to 43 years. Patients had not been previously treated with cytotoxic or immunomodulatory drugs. Patients may have been treated in the past with corticosteroids but not within 2 months of the first MR. One patient received three courses of oral prednisone (tapering down over a 10- to 12-day period from initial daily dosages of 60 or 80 mg) during the 1-year follow-up.

Each patient was observed with MR weekly for an initial period of 8 weeks, followed by a once-every-2-weeks schedule for 16 weeks and a subsequent monthly observation until the completion of 1 year. Additional imaging sessions were performed when disease activity was observed clinically or radiologically.

MR Examinations (Data Acquisition)

MR images were acquired on a 1.5-T system. Proton density–weighted and T2-weighted images were obtained using two interleaved dual-echo long-repetition-time sequences (3000/30,80/0.5 [repetition time/echo time(s)/excitations]). Contiguous 3-mm-thick sections covered the whole brain from foramen magnum to the higher convexity with an in-plane voxel size of 0.94 × 0.94 mm (24-cm field of view with a 256 × 192 acquisition matrix). Scan duration was kept at 11 minutes and 36 seconds by using the ½ Fourier technique.

Postcontrast T1-weighted (contrast-enhanced) images resulted from a 600/19/1 spin-echo sequence. Section thickness was 4 mm, with a 1-mm gap between sections. A 256 × 192 matrix was used with a 24-cm field of view. The phase-offset multiplanar (POMP) option enabled the acquisition of 24 sections. Ten milliliters of 500 mmol/L gadopentetate dimeglumine was administered intravenously immediately before the axial T1-weighted data acquisition. Identical parameters were used for an unenhanced T1-weighted sagittal localizer sequence, which was performed at the beginning of each study.

Image Analysis

Images from MR studies performed at 116 time points were analyzed. At each time point, approximately 52 double-echo and 24 contrast-enhanced sections were acquired. More than 8000 images were included in this evaluation. Newly appearing abnormalities or changes in preexisting abnormalities were detected by two neuroradiologists comparing new images with images acquired at the previous time point as well as images obtained at the first time point in the follow-up of the patient. The comparison of the baseline study with all subsequent images was performed to avoid missing subtle gradual changes, which could nevertheless result in substantial cumulative differences.

New lesions were defined as lesions not detected on the first study but seen on any subsequent proton density–weighted or contrast-enhanced studies in the series. Enhancing lesions were defined as those that demonstrated high signal, consistent with enhancement, on the contrast-enhanced images at any time in the course of the study. The location of these signal abnormalities was retrieved on each study, and the appearance of the area of the lesion was described (Figs 1 and 2). The image of a lesion at 1 time point is called a *lesion time point* (LTP) hereafter. An estimate of lesion size (largest diameter) and presence of contrast enhancement were noted. Lesion patterns were observed using display utilities of the Research Workstation image analysis software (MrX) (GE Medical Systems, Milwaukee, Wis) installed on SUN workstations (SUN Microsystems, Mountain View, Calif). After adjustment of the observable signal intensity range (level and width) such that high contrast between single pixels in the area of abnormal signal intensity was obtained, two independent readers assigned each abnormality to one of two types: central hyperintensity or ring hyperintensity. Abnormalities that could not be assigned to one of these classifications were called indeterminate in signal intensity pattern. This analysis was performed on the proton density–weighted and on the contrast-enhanced images. Unless otherwise specified, lesion age was calculated from the time of a lesion's first detection on MR, irrespective of the time elapsed since the preceding MR.

Nonparametric Wilcoxon's rank sum statistics were applied to assess the significance of noted age-dependent differences in signal intensity patterns (11). Significance probabilities (*P* values) were calculated using the normal approximation of the Wilcoxon distribution. Differences were considered significant at the .05 level. Only LTPs at which both raters agreed on the pattern classification were included in the statistical evaluation.

Results

Forty-three enhancing lesions and 1 new lesion that never enhanced during the whole period of follow-up were detected in four of the five patients examined and were followed for a total of 702 LTPs. One patient showed no new lesions during the observed period. Lesions per patient are given in the Table.

A total of 18 enhancing lesions already were present at the first time point and were therefore discarded from the age-dependent analysis of signal intensity distribution patterns. Two other lesions were discarded because both observers
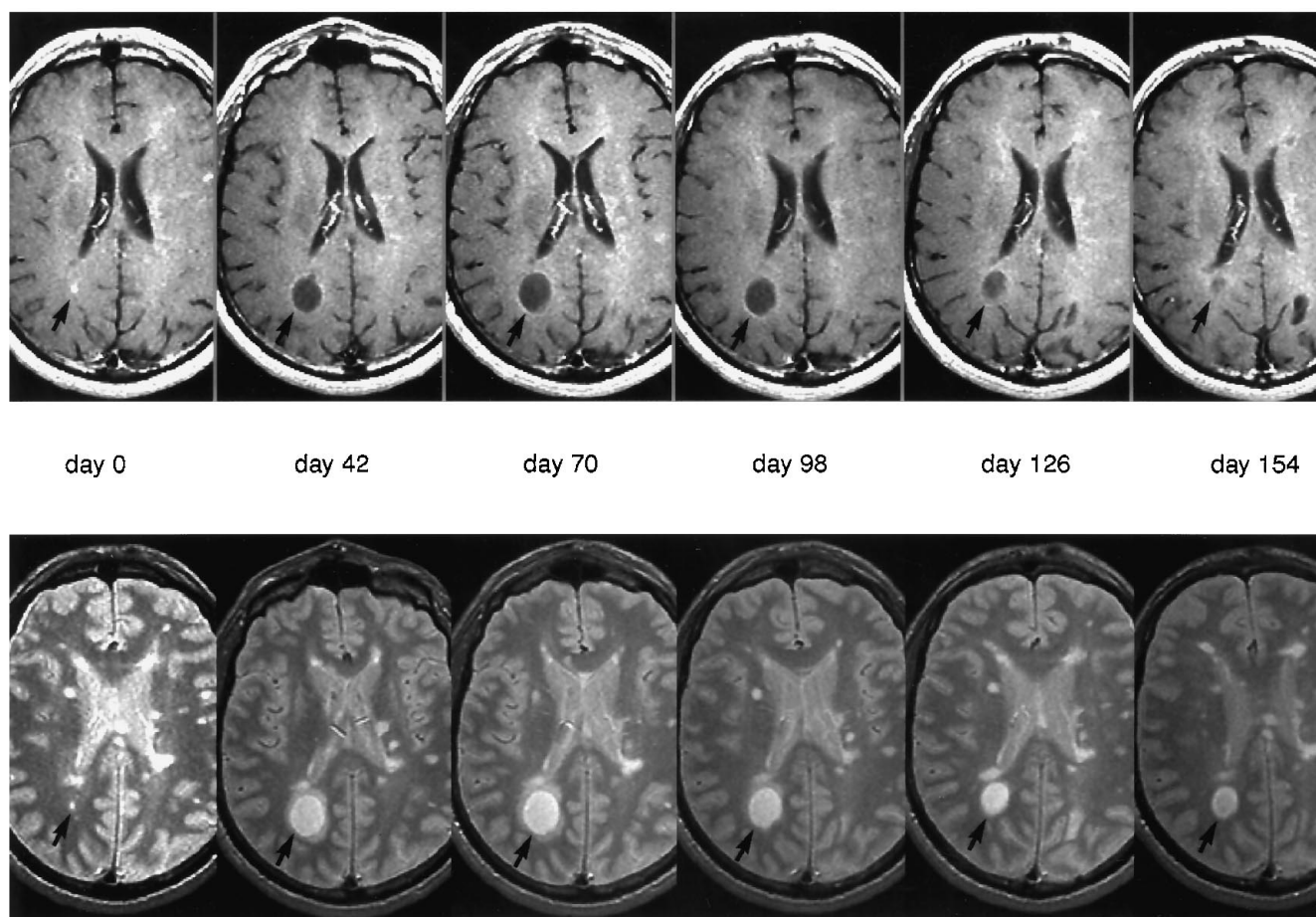
Fig 1. The life of a multiple sclerosis lesion. Serial MR follow-up of a multiple sclerosis lesion (*arrows*) in the right parietooccipital white matter of a 37-year-old man. Contrast-enhanced (*top*) and proton density–weighted (*bottom*) MR images of the brain at a comparable anatomic level are shown at the lesion's first detection and at subsequent time points. The indicated lesion age is calculated by designating time of first MR detection as day 0. The images were photographed with the signal intensity range (window and level) adjusted to enhance the contrast in the diseased white matter. A pattern of central hyperintensity can be seen on contrast-enhanced and proton density–weighted imaging at day 0. At subsequent time points and on both weightings, the lesion was seen to possess a central, darker core, surrounded by a brighter periphery, which was defined as a pattern of ring hyperintensity. Incidentally, several areas of persisting hyperintensity also are seen on these contrast-enhanced images. Most of these hyperintense areas are not consistent with contrast agent accumulation and can be correlated to areas of chronic abnormality on corresponding proton density–weighted images.

were unable to define the abnormality as one individual or two confluent focal lesions. The remaining 24 new lesions, followed over a total of 251 LTPs, were selected for the following evaluation.

Intensity Pattern of New Lesions at First Detection

On proton density–weighted images 20 of 24 new lesions were classified by both raters as having central hyperintensity pattern at the time of first detection. Two of the four remaining new lesions were classified as centrally hyperintense by only one of the two raters at their first LTP. Statistical comparison of LTPs before 30 days

with those on or after 30 days showed that the earlier LTPs demonstrated central hyperintensity classification on proton density–weighted images significantly more frequently than later LTPs ($P = .0008$). This relationship remained statistically significant ($P < .0001$) when only abnormalities with diameters greater than 4 mm were considered, to reduce bias attributable to lesion size.

On contrast-enhanced images the two raters were in agreement on classifying the newly enhancing lesions as centrally hyperintense in 19 of the 23 enhancing lesions. One other lesion was classified as centrally hyperintense by only one of the two observers. Again, central hyperintensity pattern was found to be significantly
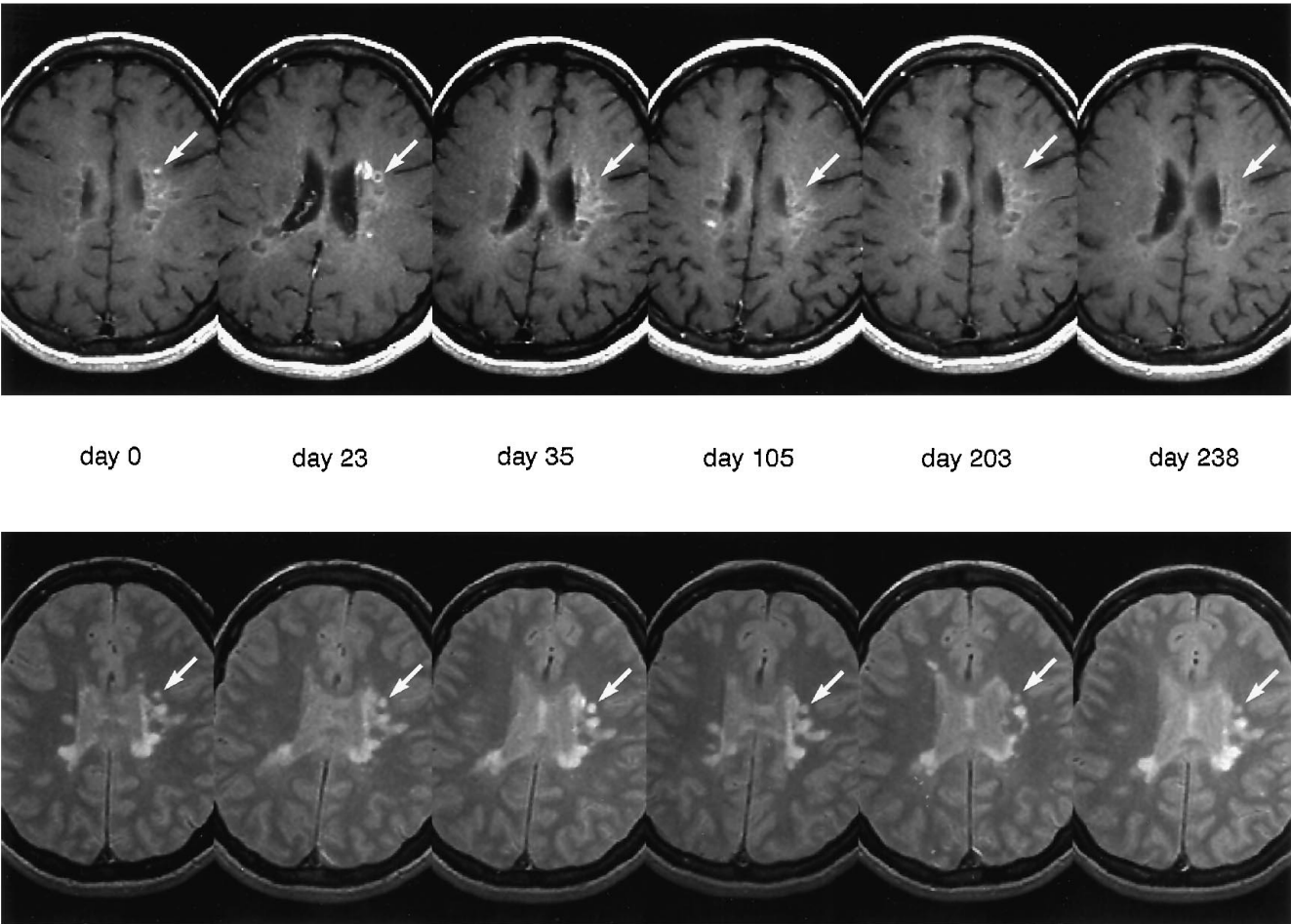
day 0   day 23   day 35   day 105   day 203   day 238

Fig 2. Signal intensity pattern changes of a multiple sclerosis lesion. A lesion (*arrows*) in the left frontal periventricular white matter of a 36-year-old woman is shown at six time points, beginning with the time of first detection (day 0) on contrast-enhanced (*top*) and proton density–weighted (*bottom*) MR images. On contrast-enhanced images, the lesion has a central hyperintensity pattern at day 0, which evolves into a clearly enhancing ring pattern 23 days later. At day 35, this lesion still presents with a pattern of ring hyperintensity, which cannot be clearly ascribed to the accumulation of contrast agent. The ring hyperintensity grows fainter and eventually disappears by day 238. On the corresponding proton density–weighted images, a central hyperintensity pattern at day 0 was followed by the appearance of ring hyperintensity, which was detected at 23, 35, and 105 days. At 203 and 238 days, central hyperintensity pattern was seen.

Five patients with relapsing-remitting multiple sclerosis

Patient	Age, y	Sex	MR Exams, n	New Lesions, n	Confluent Lesions*, n	Enhancing Lesions, n	Lesions Not Enhancing at 1st Detection on Proton Density–Weighted Images, n
A	36	F	23	7	—	13	—
B	27	F	22	1[†]	—	1	—
C	43	F	23	0	—	0	—
D	40	F	24	4	—	4	—
E	37	M	24	14	2	25	7

* New lesions appearing to be issuing from the confluence of multiple individual focal lesions were excluded from signal intensity pattern analysis.

[†] This new lesion never demonstrated contrast uptake and was detected solely on proton density–weighted images.

more frequent in lesions observed less than 30 days after first detection than at later time points ($P <$ .0001 without size cut-off, $P =$ .0005 when considering only lesions with a diameter >4 mm).

On both proton density–weighted and contrast-enhanced images, newly detected lesions showed higher signal intensity at their centers (compared with their peripheries).

Subacute and Chronic Changes in Signal Intensity Patterns

We wanted to know what proportion of these lesions show a change in pattern (ie, change from central hyperintensity to ring hyperintensity and/or indeterminate) in the course of their

evolution. We considered a change in pattern to be "true" only if both observers noted one at the same time point and assigned identical classification. With this stringency, 13 of the 20 lesions unanimously classified as central hyperintensity at the time of appearance on proton density–weighted images subsequently changed their signal intensity pattern to ring hyperintensity (7 lesions) and/or to indeterminate (8 lesions). Two of the remaining seven lesions with initial central hyperintensity but subsequently unchanged pattern on proton density–weighted images were followed for only 28 days, because they were detected close to the end of the 1-year follow-up period. Three other unchanging lesions maintained a 2-mm diameter during the course of follow-up. Anec-
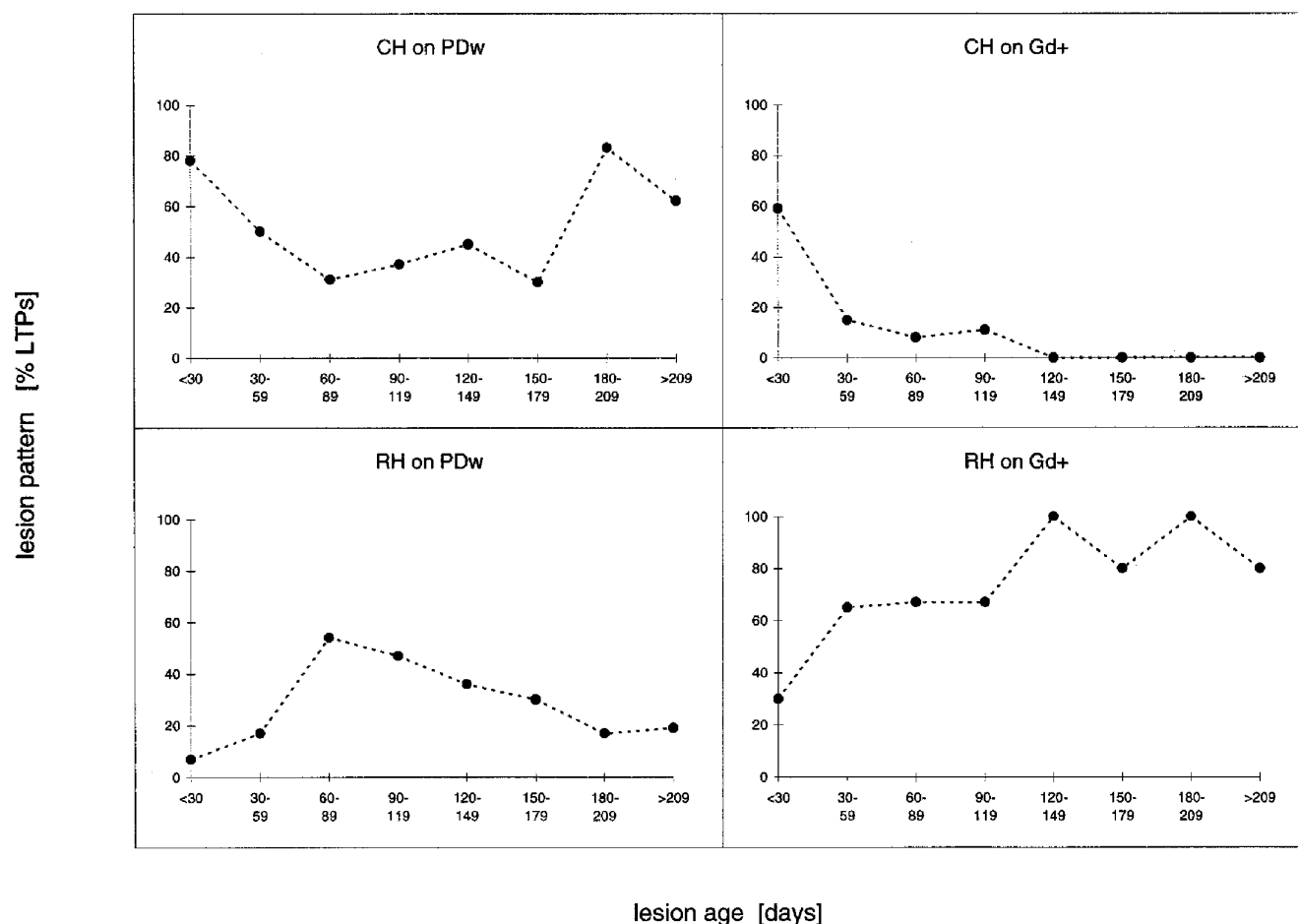

Fig 3. Age-dependent distribution of lesion signal intensity patterns. Scatter plots of all LTPs that were assigned the same signal intensity pattern by both raters (*CH* indicates central hyperintensity, *RH* indicates ring hyperintensity). The distribution of assigned patterns is shown as a function of lesion age. Time points were grouped in intervals of 1 month (30 days). Each point represents the fraction of time points in a given age interval that was classified by both raters as central hyperintensity (*CH, top*) or ring hyperintensity (*RH, bottom*). This analysis was performed on proton density–weighted (*PDw, left*) and contrast-enhanced (*Gd+, right*) images. The interpolation (*dashed line*) is shown for better visualization of the trends.

dotally, it might be of interest to note that two of these three lesions were under oral prednisone treatment during the first 2 weeks after detection. Of the 7 lesions that changed to ring hyperintensity, only one reverted to a central hyperintensity pattern. Figure 3 is a representation of the signal intensity pattern distribution of LTPs as a function of their age and includes all time points of the evaluated lesions for which the raters were concordant in their pattern classification. From Figure 3, it appears that on proton density–weighted images, the fraction of LTPs with a central hyperintensity pattern decreases to reach a minimum between 2 and 4 months of age. The difference between the frequency of central hyperintensity patterns in this 2-month period and both that in the first 2 months after lesion detection (P = .0021 [no size cutoff] and P = 0.0014 [lesions >4 mm]) and that after 179 days (P = .0170 [no size cutoff] and P = .0322 [lesions >4 mm]), was statistically significant. There was no statistically significant difference between 2- to 4-month old and 4- to 6-month-old abnormalities (P = .409 [no size cutoff] and P = .0918 [lesions >4 mm]).

The inverse was true for the ring hyperintensity pattern: its frequency increased to peak in LTPs between 60 and 119 days (Fig 3). In this interval, ring hyperintensity was more frequent than it was before 60 days (P = .0006 [no size cutoff] and P < .0001 [lesions >4 mm]) and after 179 days (P = .0197 [no size cut off] and P = .0154 [lesions >4 mm]). The group of observations between 120 and 179 days demonstrated a statistically significant difference in the proportion of ring hyperintensity patterns when lesions 4 mm or smaller (ie, less than 5 pixels in diameter) were excluded (P = .0154). Statistically significant difference with the latter age group was not seen without the size cutoff (P = .1562).

On contrast-enhanced images, 15 of 19 lesions changed from central hyperintensity to ring hyperintensity (9 lesions) and/or indeterminate (9 lesions) patterns. Some lesions showed a bright rim (ring hyperintensity pattern) that was not ascribed to gadopentetate dimeglumine accumulation and persisted long after enhancement had subsided. The general trend is one of transition from a majority of centrally hyperintense early LTPs to later ones showing a predominant pattern of ring hyperintensity (Fig 3 and Fig 5). LTPs after 1 month

presented a centrally hyperintense pattern on contrast-enhanced images in only approximately 10% of the cases (Fig 3). Ring hyperintensity pattern was significantly more frequent in LTPs after 29 days than on or before 29 days (P < .0001 [no size cutoff] and P = .0026 [lesions >4 mm]) (Fig 4).

The time course of two lesions is depicted in Figures 1 and 2. Both raters agreed on classifications in 158 (64%) of 247 LTPs on proton density–weighted images (lesions were not seen by one or both raters in 4 of 251 follow-up LTPs) and 112 (77.8%) of 144 LTPs on contrast-enhanced images.

Lesion Size

The next question we addressed was the influence of lesion size on classification. A measure of lesion size was given by estimating the largest diameter. Not surprisingly, smaller lesions were classified much more frequently as having a pattern of central hyperintensity on proton density–weighted images: in 93.9% of all LTPs at which lesions were smaller than 4 mm (major diameter), they were considered centrally hyperintense. We therefore computed all statistics with and without inclusion of LTPs at which lesions had maximal diameter 4 mm and smaller. The overall conclusions reached above remained true even after exclusion of these LTPs of smaller lesions. On average, lesions reached their maximum diameter on proton density–weighted images at about 26.9 days after their first detection on MR.

Contrast Enhancement

Duration of gadopentetate dimeglumine enhancement was estimated for each observed lesion (Fig 5). The longest period of enhancement in a lesion appeared to be 98 days after first detection on MR. On average, the latest observation of contrast enhancement was 31.9 days after first detection of a new lesion on MR. The average interval between the last exam demonstrating contrast enhancement in a lesion and the subsequent nonenhancing exam was 20.6 days. The average interval between the first exam demonstrating contrast enhancement in a lesion and the previous nonenhancing exam was 23 days.

Ring hyperintensity can be present on unenhanced T1-weighted images and was frequently
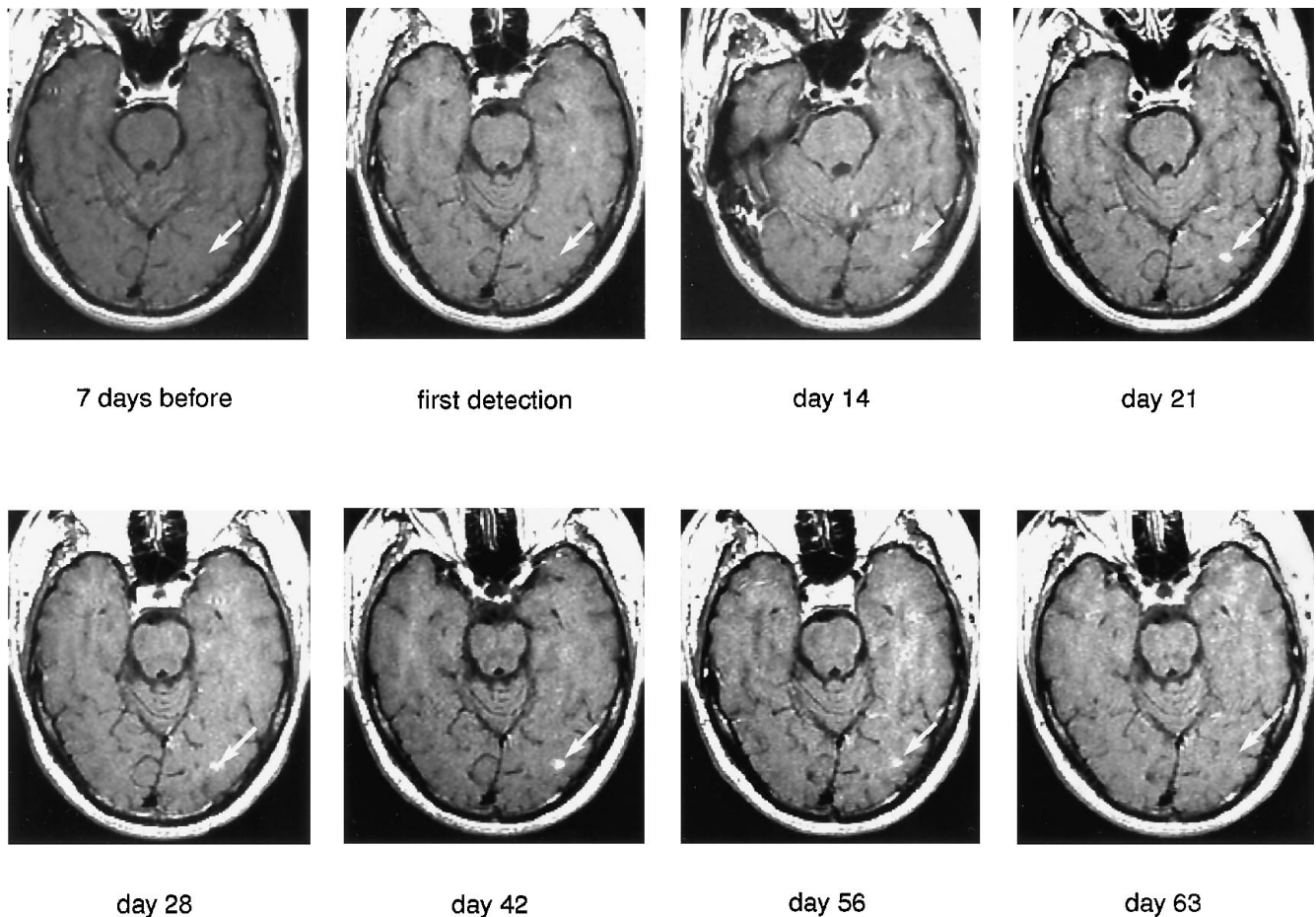
Fig 4. Duration of contrast enhancement in a new multiple sclerosis lesion. The location of a lesion (*arrow*) is retrieved on sequential contrast-enhanced studies of a 37-year-old man. Definite enhancement is seen on all studies from the day of first detection (day 0) to day 56. No contrast accumulation was detected at the location of this lesion 7 days before or 7 days after this interval. The duration of enhancement of this lesion is typical of the average duration of enhancement of multiple sclerosis lesions, which was found to be between 1 and 2 months.

observed on our T1-weighted sagittal localizer images. Figure 6 shows examples of "ring" lesions on unenhanced T1-weighted images that persisted over the whole year of follow-up. Eleven lesions on contrast-enhanced and 10 lesions on proton density–weighted images demonstrated ring hyperintensity also at time points without evident contrast enhancement of the lesion.

Discussion

The results presented here indicate consistency in the pattern of presentation of newly appearing lesions on MR, namely a pattern of central hyperintensity. This was seen in the majority of new lesions, both on proton density– and contrast-enhanced T1-weighted images.

A large proportion of these lesions showed changes in signal intensity pattern in the course of follow-up. The sequence and timing of these pattern changes, however, were not consistent, and we were unable to determine a clear-cut model for the course of evolution of these lesions, as seen on MR. Nevertheless, an average lesion course can be inferred in the framework of current neuropathologic and neuroradiologic knowledge, the need for further experimental confirmation notwithstanding.

One of the earliest steps in lesion formation is the breakdown of the blood-brain barrier, which translates into high signal on proton density–weighted as well as on contrast-enhanced images (12, 13). It has been proposed that the blood-brain barrier breakdown in multiple sclerosis is related primarily to perivenular astro-
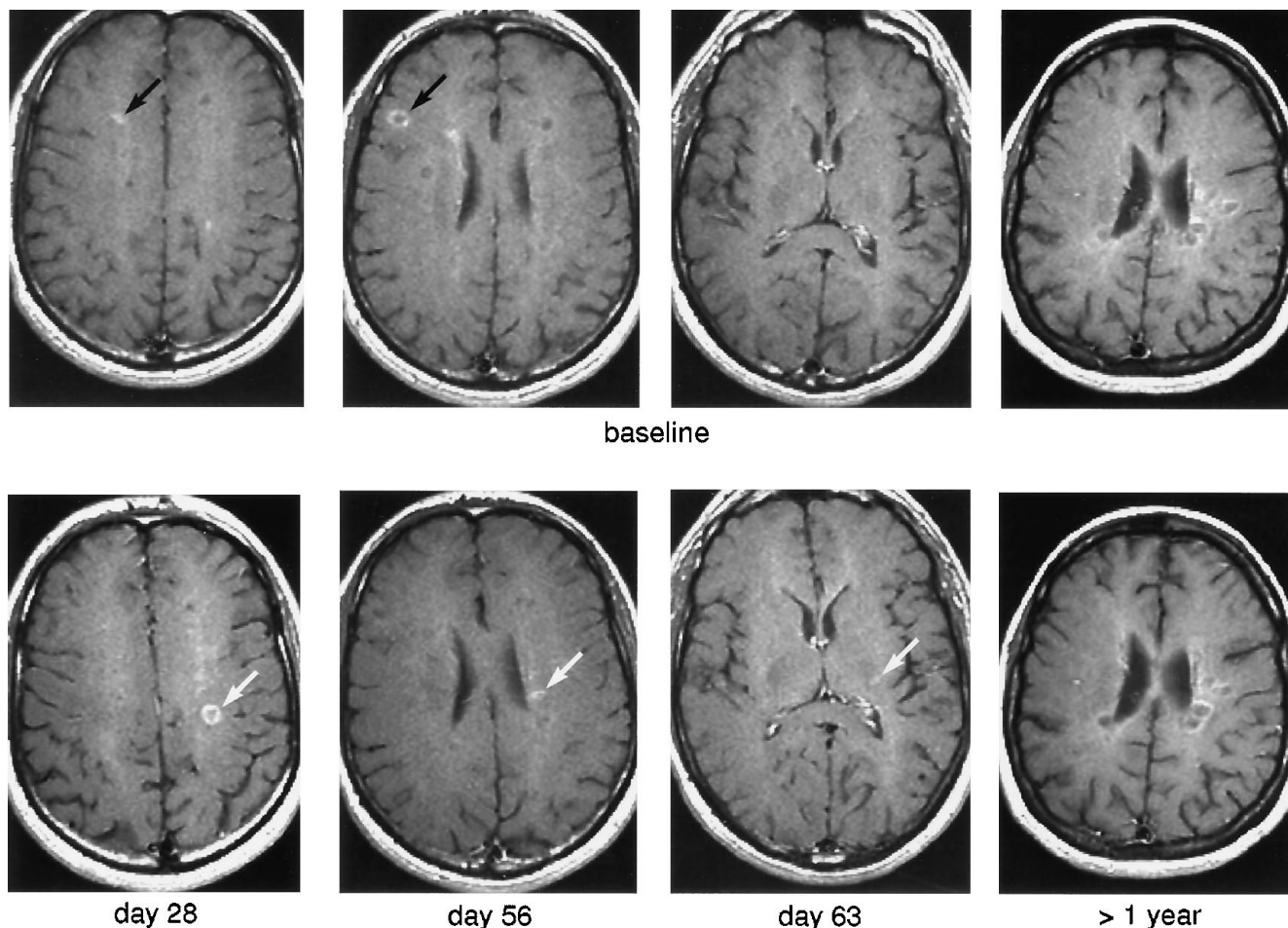
Fig 5. Ring hyperintensity pattern of multiple sclerosis lesions on contrast-enhanced MR images. Ring hyperintensity is shown in lesions at different times in their evolution. The *white arrows* indicate lesions that appeared during the course of follow-up (ages since first detection are annotated at the bottom); whereas the ring hyperintensity in the 28- and 56-day-old lesions was ascribed to the accumulation of contrast agent, this was not the case for the 63-day-old lesion. On the far right, several ring lesions are shown that presented a pattern virtually identical to that on the baseline study more than 1 year later. In the top row, as comparison, are images at comparable anatomic location from the first study in the patient's follow-up (ie, baseline). Two enhancing lesions are indicated by *black arrows*. Their ages are unknown, because no prior study was obtained. They were therefore excluded from our statistical evaluation.

cytic damage, while sparing the vascular endothelium of the venules, which are typically located in the center of lesions (6, 14). An alternate view involves functional impairment of morphologically intact endothelial cells showing increased pinocytotic activity (15). In both scenarios, the considerable swelling of astroglia and endothelium accompanying this phenomenon is likely to reinforce early T2 prolongation because of local increase of water content (16). Oligodendrocyte damage, which is of central relevance in the development of nerve-conduction impairment and therefore of neurologic symptoms (17), also appears to be a very early event of lesion formation (5). The ensuing demyelination appears to progress over a period of several weeks, typically by contiguous spread irrespective of nerve fiber orientation (6). This process is accompanied by the appearance of swollen oligodendroglia, cellular infiltration (lymphocytes and lipid-engulfing macrophages known as Gitter cells), and expansion of the extracellular spaces, as evidenced by optical as well as electron microscopic studies of multiple sclerosis plaques (6, 18–20). Increased signal on long-repetition-time images is consistent with these phenomena (21–23). The pattern of central hyperintensity we observed on proton density–weighted images in the early course of multiple sclerosis lesion formation may therefore be tentatively ascribed to the combined influences of increased extracellular and intracellular spaces (demyelination and inflammatory cell swelling and infiltration)

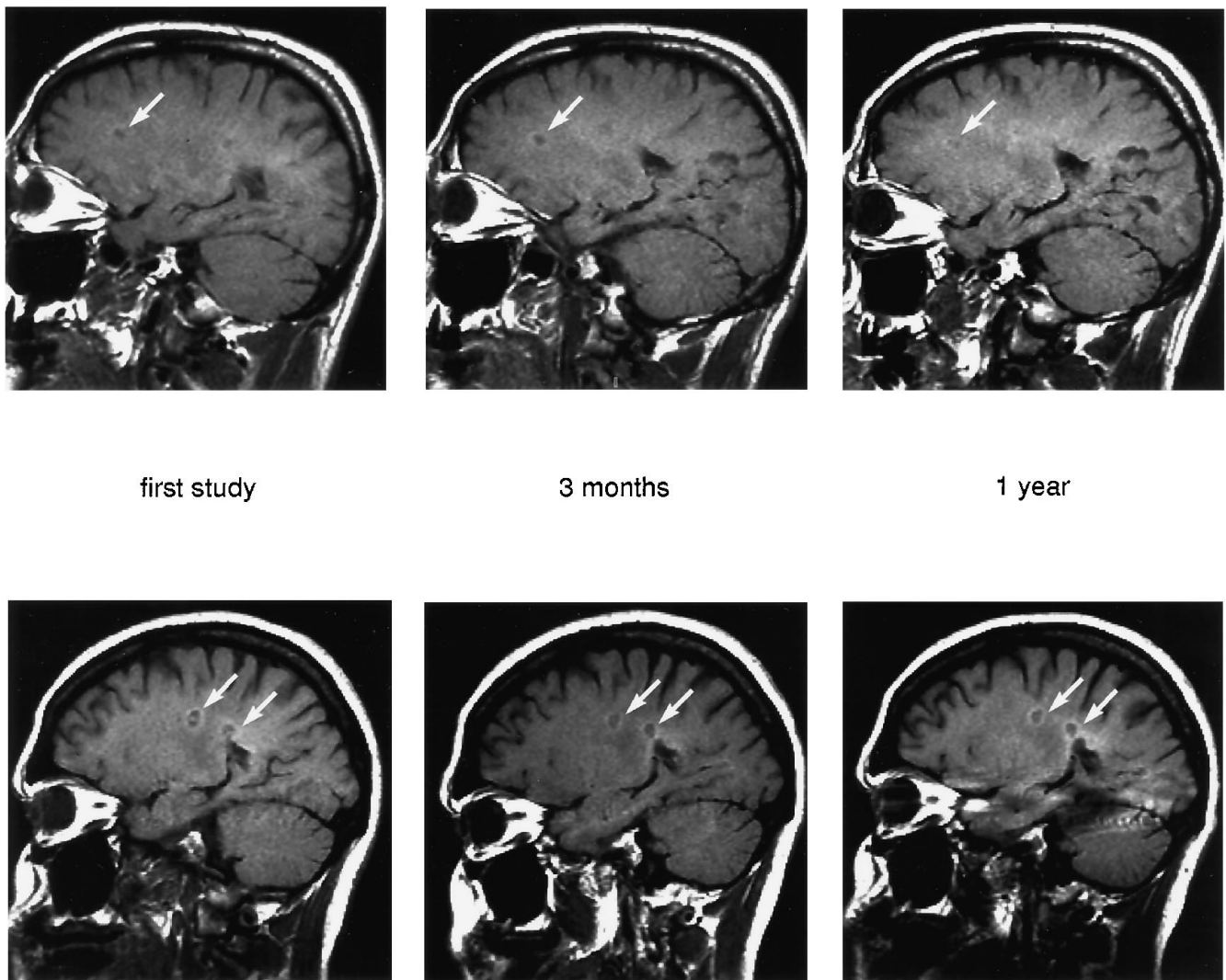first study   3 months   1 year

Fig 6. Ring hyperintensity pattern of multiple sclerosis lesions on unenhanced T1-weighted MR images. Ring hyperintensity can be detected on unenhanced T1-weighted MR images and can remain visible for at least 1 year. Three lesions (*white arrows*) on sagittal images of the brains of two different patients are shown on the first study, as well as 3 months and 1 year later. The pattern of ring hyperintensity is maintained at all these time points.

concomitant with a decrease in the fraction of faster-relaxing bound water associated with the decrease in biomembrane surfaces. The pattern of central contrast enhancement on contrast-enhanced images may reflect the impairment of the blood-brain barrier at the central venule and/or capillary levels, indicating either blood-brain barrier breakdown as a consequence of a multiple sclerosis–specific primary damage or secondary to a primarily intraparenchymatous inflammatory reaction.

After the progressive and centrifugal disappearance of oligodendrocytes, fibrillary astrocytosis and bouts of remyelination fill the gaps. T2 shortening can be expected to accompany these phenomena, because of local decrease in water content and increased water immobilization by increasing membrane surfaces (16). This would fit the appearance of relatively dark lesion centers on proton density–weighted images in a phase of lesion evolution at which active inflammation and demyelination at the lesion's outer bounds coexist with repair processes at its pathogenetically older center (Figs 1 and 2). This ring shape appeared to peak for the average lesion around the age of 3 months (see Fig 3).

Ring enhancement has been previously described (2, 12, 24–26). However, to our knowledge, no conclusive explanation has been pro-

vided for the mechanism of how the contrast reaches the lesion margin. It appears unlikely for a central venule to be the origin of such leakage, as appears to be the case in acute lesions. We speculate that the distribution pattern of contrast agent in older lesions, with peripheral inflammatory activity, rather could be ascribed to secondary capillary hyperemia and/or damage. This view is consistent with histopathologic findings of capillary alterations in multiple sclerosis plaques (15) and is also supported by dynamic MR studies of contrast accumulation in multiple sclerosis lesions, which demonstrated initial ring enhancement with subsequent filling in of the central disk (27). Following this hypothetical model, it can be expected that ring hyperintensity on proton density–weighted images, reflecting peripheral enlargement of the extracellular space around freshly demyelinated naked nerve fibers and presence of inflammatory and reactive cells, would be apparent longer than contrast enhancement on contrast-enhanced images, symptomatic of a leaking blood-brain barrier. Indeed, this sequence of events was apparent in 10 of the lesions we followed for a sufficient period of time. These were seen as ring hyperintensity on proton density–weighted images, whereas at the same time no enhancement was detected on contrast-enhanced images. Our data on duration of enhancement are consistent with previous reports (24, 28–30). No lesion showed enhancement later than 14 weeks after detection, in agreement with the report by Harris et al (28). Given the average length of observed gadopentetate dimeglumine enhancement (31.9 days) and the average length of "blind" intervals between first enhancing exam and previous nonenhancing exam (23 days) and between last observed enhancement and subsequent negative follow-up exam (20.6 days), we estimate that new multiple sclerosis lesions demonstrate gadopentetate dimeglumine uptake for 1 to 2 months on average. Several authors have described a pattern of ring hyperintensity on unenhanced T1-weighted images and suggested the presence of free radicals in infiltrating macrophages as the likely cause (2, 31, 32). In 11 lesions, we observed ring hyperintensity on postcontrast T1-weighted images that was not ascribed to contrast leakage. This pattern persisted long after cessation of evident enhancement attributable to the contrast agent and even in lesions older

than 200 days (Figs 5 and 6). We also observed multiple lesions on unenhanced T1-weighted images that persisted with a ring hyperintensity pattern for at least 1 year (Fig 6). It is questionable that the sustained presence of this pattern should be ascribed solely to the macrophage activity. Further evaluation would be needed to associate unequivocally such long-term persistence of hyperintense rims on unenhanced T1-weighted images with the presence of free radicals in active macrophages, and alternate explanations should be explored. These observations, however, underline the potential importance of unenhanced T1-weighted images for complete lesion characterization in imaging protocols of therapeutic trials involving immunomodulatory drugs that might influence phagocytic activity.

On proton density–weighted and contrast-enhanced images, a majority of lesions were centrally hyperintense at early time points and subsequently changed pattern of appearance in the course of follow-up. On proton density–weighted images, ring hyperintensity was most frequent at LTPs 2 to 4 months (60 to 119 days) after lesion detection. Ring hyperintensity was seen at the majority of LTPs after 1 month on contrast-enhanced images. It was estimated that new multiple sclerosis lesions demonstrate gadopentetate dimeglumine uptake, on average, during a period of 1 to 2 months. The hyperintensity on contrast-enhanced images was not always ascribed to gadopentetate dimeglumine accumulation, and ring hyperintensity was chronically detected during a whole year on unenhanced T1-weighted images as well. These data appear consistent with current neuropathologic knowledge. We believe that, with further experimental evaluation, specific information about the histopathologic evolution of multiple sclerosis lesions could be extracted not only from contrast-enhanced but also from nonenhanced serial MR. This information could be of use in the evaluation of treatments targeting specific pathogenetic components of multiple sclerosis.

Acknowledgments

References

1. Katz D, Taubenberger J, Raine C, McFarlin D, McFarland H. Gadolinium-enhancing lesions on magnetic resonance imaging: neuropathological findings. *Ann Neurol* 1990;28:243

2. Nesbit GM, Forbes GS, Scheithauer BW, Okazaki H, Rodriguez M. Multiple sclerosis: histopathologic and MR and/or CT correlation in 37 cases at biopsy and three cases at autopsy. *Radiology* 1991;180:467–474

3. Estes ML, Rudick RA, Barnett GH, Ransohoff RM. Stereotactic biopsy of an active multiple sclerosis lesion: immunocyto-chemical analysis and neuropathologic correlation with magnetic resonance imaging. *Arch Neurol* 1990;47:1299–1303

4. Newcombe J, Hawkins CP, Henderson CL, et al. Histopathology of multiple sclerosis lesions detected by magnetic resonance imaging in unfixed postmortem central nervous system tissue. *Brain* 1991;114:1013–1023

5. Rodriguez M, Scheithauer BW, Forbes G, Kelly PJ. Oligodendrocyte injury is an early event in lesions of multiple sclerosis. *Mayo Clin Proc* 1993;68:627–636

6. Lumsden CE. The neuropathology of multiple sclerosis. In: Vinken PJ, Bruyn GW (eds). *Handbook of Clinical Neurology.* Amsterdam: North-Holland Publishing Co, 1970;9:217–309

7. Hawkins CP, Munro PMG, MacKenzie F, et al. Duration and selectivity of blood-brain barrier breakdown in chronic relapsing experimental allergic encephalomyelitis studied by gadolinium-DTPA and protein markers. *Brain* 1990;113:365–378

8. Raine CS. Multiple sclerosis and chronic relapsing EAE: comparative ultrastructural neuropathology. In: Hallpike JF, Adams CWM, Tourtellotte WW (eds). *Multiple Sclerosis: Pathology, Diagnosis and Management.* Baltimore: Williams & Wilkins, 1983: 413–460

9. Shaw CM, Alvord EC, Jr. A morphologic comparison of three experimental models of experimental allergic encephalomyelitis with multiple sclerosis. In: Alvord EC Jr, Kies MW, Suckling AJ (eds). *Experimental Allergic Encephalomyelitis: A Useful Model for Multiple Sclerosis.* New York: Alan R Liss, Inc, 1984:61–66

10. Grossman RI, Lisak RP, Macchi PJ, Joseph PM. MR of acute experimental allergic encephalomyelitis. *AJNR Am J Neuroradiol* 1987;8:1045–1048

11. Lehmann EL. Nonparametrics: statistical methods based on ranks. New York: McGraw-Hill, 1975:1–23

12. Grossman RI, Gonzalez-Scarano F, Atlas SW, Galetta S, Silberberg DH. Multiple sclerosis: gadolinium enhancement in MR imaging. *Radiology* 1986;161:721–725

13. Kermode AG, Thompson AJ, Tofts PS, et al. Breakdown of the blood-brain barrier precedes symptoms and other MR signs of new lesions in multiple sclerosis: pathogenetic and clinical implications. *Brain* 1990;113:1477–1489

14. Broman T. Blood-brain barrier damage in multiple sclerosis: supra-vital test observations. *Acta Neurol Scand* 1964;40(Suppl 10):21–24

15. Brown WJ. The capillaries in acute and subacute multiple sclerosis plaques: a morphometric analysis. *Neurology* 1978;28:84–92

16. Cameron IL, Ord VA, Fullerton GD. Characterization of proton NMR relaxation times in normal and pathological tissues by correlation with other tissue parameters. *Magn Reson Imaging* 1984; 2:97–106

17. Namerow NS. The pathophysiology of multiple sclerosis. In: Wolfgram F, Ellison GW, Stevens JG, Andrews JM (eds.). *Multiple Sclerosis: Immunology, Virology, and Ultrastructure (UCLA Forum in Medical Sciences, Number 16).* New York and London: Academic Press, 1972;16:143–172

18. Traugott U, Reinherz EL, Raine CS. Multiple sclerosis distribution of T-cells, T-cell subsets, and la-positive macrophages in lesions of different ages. *J Neuroimmunol* 1983;4:201–221

19. Olvera-Rabiela JE, Rabiela-Cervantes MT, Feria-Velasco A, Marquez-Padilla H, González-Angulo A. Multiple sclerosis in Mexico: light- and electron-microscopic study of two cases. *Neurology* 1971;21:720–727

20. Périer O, Grégoire A. Electron microscopic features of multiple sclerosis lesions. *Brain* 1965;88:937–952

21. Teresi LM, Hovda D, Seeley AB, Nitta K, Lufkin RB. MR imaging of experimental demyelination. *AJNR Am J Neuroradiol* 1989;10: 307–314

22. Jolesz FA, Polak JF, Ruenzel PW, Adams DF. Wallerian degeneration demonstrated by magnetic resonance: spectroscopic measurements on peripheral nerve. *Radiology* 1984;152:85–87

23. Jolesz FA, Polak JF, Adams DF, Ruenzel PW. Myelinated and nonmyelinated nerves: comparison of proton MR properties. *Radiology* 1987;164:89–91

24. Miller DH, Rudge P, Johnson G, et al. Serial gadolinium enhanced magnetic resonance imaging in multiple sclerosis. *Brain* 1988; 111:927–939

25. Barkhof F. *Gadolinium Enhanced Magnetic Resonance Imaging in Multiple Sclerosis.* Amsterdam: VU University Press; 1992

26. Capra R, Marcianò N, Vignolo LA, Chiesa A, Gasparotti R. Gadolinium-pentetic acid magnetic resonance imaging in patients with relapsing remitting multiple sclerosis. *Arch Neurol* 1992;49:687–689

27. Kermode AG, Tofts PS, Thompson AJ, et al. Heterogeneity of blood-brain barrier changes in multiple sclerosis: an MR study with gadolinium-DTPA enhancement. *Neurology* 1990;40:229–235

28. Harris JO, Frank JA, Patronas N, McFarlin DE, McFarland HF. Serial gadolinium-enhanced magnetic resonance imaging scans in patients with early, relapsing-remitting multiple sclerosis: implications for clinical trials and natural history. *Ann Neurol* 1991; 29:548–555

29. Koopmans RA, Li DKB, Oger JJF, Mayo J, Paty DW. The lesion of multiple sclerosis: imaging of acute and chronic stages. *Neurology* 1989;39:959–963

30. Grossman RI, Braffman BH, Brorson JR, et al. Multiple sclerosis: serial study of gadolinium-enhancing MR imaging. *Radiology* 1988;169:117–122

31. Drayer BP. Magnetic resonance imaging of multiple sclerosis. *Barrow Neurol Inst Q* 1987;3:65–73

32. Powell T, Sussman JG, Davies-Jones GAB. MR imaging in acute multiple sclerosis: ringlike appearance in plaques suggesting the presence of paramagnetic free radicals. *AJNR Am J Neuroradiol* 1992;13:1544–1546